Capillary Force Driven Self-Assembly of Anisotropic Hierarchical Structures Prepared by Femtosecond Laser 3D Printing and Their Applications in Crystallizing Microparticles

Zhaoxin Lao, Yanlei Hu, Chenchu Zhang, Liang Yang, Jiawen Li,* Jiaru Chu, and Dong Wu*

CAS Key Laboratory of Mechanical Behavior and Design of Materials, Department of Precision Machinery and Precision Instrumentation, University of Science and Technology of China, Hefei, Anhui 230027, China

ABSTRACT The hierarchical structures are the derivation of various functionalities in the natural world and have inspired broad practical applications in chemical systhesis and biological manipulation. However, traditional top-down fabrication approaches suffered from low complexity. We propose a laser printing capillary-assisted self-assembly (LPCS) strategy for fabricating regular periodic structures. Microscale pillars are first produced by the localized femtosecond laser polymerization and are subsequently self-assembled into periodic hierarchical architectures with the assistance of controlled capillary force. Moreover, based on anisotropic assemblies of micropillars, the LPCS method is further developed for the preparation of more complicated and advanced functional microstructures. Pillars cross section, height, and spatial arrangement can be tuned to guide capillary force, and diverse assemblies with different configurations are thus achieved. Finally, we developed a strategy for growing micro/nanoparticles in designed spatial locations through solution-evaporation self-assembly induced by morphology. Due to the high flexibility of LPCS method, the special arrangements, sizes, and distribution density of the micro/nanoparticles can be controlled readily. Our method will be employed not only to fabricate anisotropic hierarchical structures but also to design and manufacture organic/inorganic microparticles.

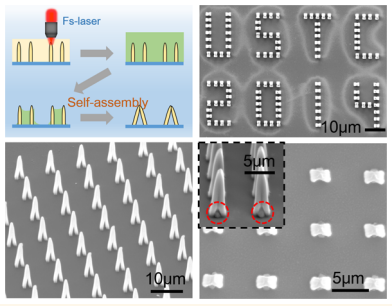

KEYWORDS: self-assembly · capillary force · femtosecond laser · hierarchical structures · microparticles

Controllable preparation of ordered complex micro/nano hierarchical architectures in a controlled fashion is of great importance to current scientific research and technical implementations.[1] Many top-down technologies, such as ultraviolet (UV) photolithography,[2] electron beam lithography (EBL),[3] focused-ion-beam (FIB),[4] were already well established and have been widely used to fabricate micro/nanostructures.[5] These methods can produce well-designed structures which are relatively simple. However, in order to fabricate complex 3D structures, complex multistep processing should be relied on in these methods.[6] Generally, both high complexity and large-area are demanded for practical applications, and conventional top-down approaches fail to fulfill these requirements because of their limited efficiency and long-range ability. Especially, many top-down approaches rely on complicated multistep processes when manufacture a complex structure, which is neither simple nor economic. Therefore, the bottom-up approach, which can assemble various complex microstructures from small solid components or molecules, has emerged as a promising tool for large-scale hierarchical structures preparation.[5,7,8]

Though much higher efficiency can be achieved by bottom-up approach compared with conventional top-down nanomanufacturing methods, its regularity and controllability are a little poor. As an ingenious strategy, the combination of top-down/bottom-up technologies to realize controllable micro/nanostructures has become a hot topic since it can produce a lot of functional microarchitectures which are difficult

* Address correspondence to jwl@ustc.edu.cn, dongwu@ustc.edu.cn.

Received for review August 7, 2015 and accepted October 27, 2015.

Published online October 27, 2015
10.1021/acsnano.5b04914

to obtain by a single technique.[9] Until now, a variety of regular complex 3D microarchitectures, for example, ZnO flower arrays,[10] colloidal sphere spiral chains,[11] polymer microwires,[12] and microgripper,[13−15] have been realized.

Self-assembly can be driven by weak forces, such as van der Waals forces,[16] capillary forces,[1,17] surface tension,[18,19] and internal stress between bilayers.[13,20−23] Among these, capillary force driven self-assembly has attracted great attention due to many advantages, for example, low cost, simplicity, and scalability. Many works have been done on the combination of capillary force self-assembly and top-down techniques.[1,17,24−28] For example, Pokroy *et al.*[29] reported hierarchical helical arrays by capillary force assembly of micropillar arrays, which were fabricated by the two-step soft transfer of a silicon template prepared by UV lithography and plasma etching. However, these methods are either high-cost because of the expensive equipment or labor intensive and time-consuming due to the multistep patterning and etching procedure. Wu *et al.*[9] fabricated micropillars by multibeam interference and assembled them to 3D structures with capillary force. Although multibeam interference can process large-area structures, the shape and distribution of micropillars cannot be arbitrarily designed/controlled because the interference patterns are limited, which shows low controllability and flexibility. Therefore, it is important to develop a simple and economic method for scalable fabrication of various complex micro/nanostructures for potential applications.

In addition, solution-evaporation self-assembly induced by morphology is another artful bottom-up method to manufacture micro/nanoparticles and lines.[30] However, it is also challenging to control the spatial position of material growth and deposition from solution on a surface with bottom-up synthesis of structures at the nano- and microscale.[31] To solve this problem, solution-evaporation self-assembly guided by morphology is a promising approach. Utilizing micropillar arrays made by lithography which can exhibit superhydrophobic property by the following chemical modification, micro/nanostructures could assemble at the top of the pillars.[32−37] Adopting this technology, Su *et al.* manufactured NaCl, PS, protein and Ag microparticles on the flat top surface of micropillars[36] as well as micro/nanolines.[32−35] Hatton, B. D. grew uniform $CaCO_3$ nanoparticles at the top of micropillars and controlled their sizes through concentration of liquid and time of growth.[31] Though these methods can obtain micro/nanoparticles which have relative uniform size, their dependence of chemical modification will raise the complexity of experiments as well as the quantity of equipment.

Laser printing is a flexible and simple technique to fabricate 3D microstructures.[38,39] Our group proposed a new strategy that utilize laser printing together with elastocapillary interaction for producing designable fibrillar assemblies,[40] which exhibits great flexibility and high reliability as the prepared assemblies possess controllable shapes and stable configurations. Generally, the cross section of micropillars was designed as round which formed symmetric force. In this paper, we further develop this method for preparation of anisotropic hierarchical structures. Here the cross section of the micropillars is designed to be ellipse in order to introduce asymmetric capillary forces in latitudinal and longitudinal directions and thereby guide subsequent collapse. Moreover, in previous reports, the hierarchical microstructures were only used to trap/release microparticles with different sizes which were determined by the period of the microstructures. Here, we develop a new method to grow micro/nanoparticle arrays in designed spatial position based on the employment of solution-evaporation self-assembly induced by structures that assembled by capillary force. The size and distribution density of the patterning microparticles arrays are tunable by adjusting the distribution of the micropillars assemblies or the concentration of the crystallization mother liquid. Different kinds of microparticles arrays, including NaCl, $CaCO_3$, and glucose, are successfully generated, suggesting that our approach has good universality. The combination of femtosecond laser (fs-laser) printing technique and self-assembly contained capillary-driven self-assembly and solution-evaporation self-assembly in our approach lead to a simple, rapid, flexible, facile strategy to prepare microstructures and micro/nanoparticles, which will be useful in many fields such as manufacture of hierarchical structures, fabrication of micro/nanoparticles, biological carrier, and chemical catalysis.

RESULTS AND DISCUSSION

Laser Printing of Anisotropic Micropillar Arrays. As schematically shown in Figure 1a, micropillars are readily fabricated by focusing a femtosecond laser beam into a photosensitive polymer using an objective lens. The photopolymer is mounted on a 3D nanotranslation stage to determine the pillars location and height as well as their cross section. Figure 1b shows two different cross section designs: round and ellipse. For the pillars with round cross section, the capillary force is isotropic, and direction of collapse depends only on the spatial distribution. For the pillars with ellipse cross section, the capillary force exerted on them is anisotropic, which results in directed collapse along short axis. Scanning electron microscope (SEM) images show that the axes of the ellipse cross section are 760 nm and 2 μm, respectively. The height of the pillars is 7.5 μm.

Anisotropic Self-Assembly Driven by Capillary force. The self-assembled structure is a result of competition between capillary force (F_c) and standing force (F_s) (as shown in Figure 2a). Here we define that a regular structure consists of two collapsed micropillars as a cell.

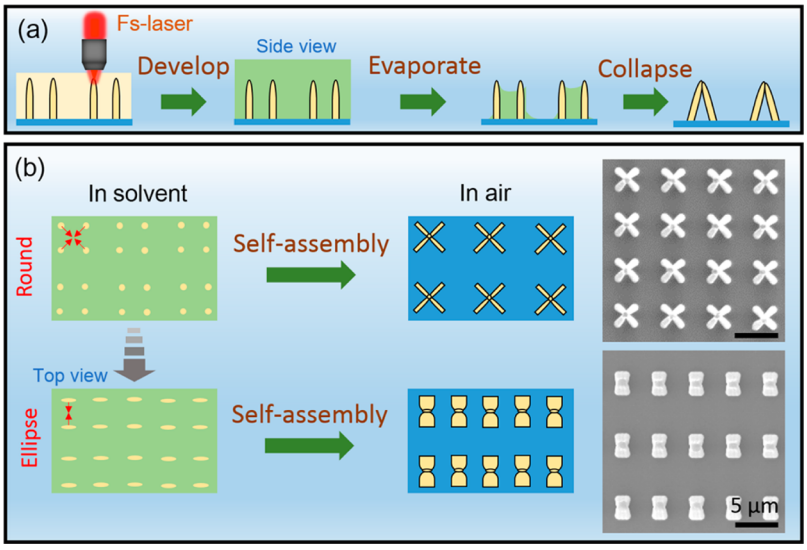

Figure 1. Scheme of capillary force induced self-assembly of laser printed isotropic and anisotropic micropillars. (a) Micropillars are fabricated by laser printing and subsequently developed in 1-propanol. Asymmetric capillary force will arise when the liquid surface reaches the tips of micropillars appearing in evaporation process, which leads to collapse of the micropillars. (b) The cross section of micropillars has two different designs: round or ellipse. When it is round, the capillary force can only be guided by the distribution of micropillars. For micropillars with ellipse cross section, the force on a single pillar is asymmetric which leads to the collapse in the direction of short axis. Scale bars: 5 μm.

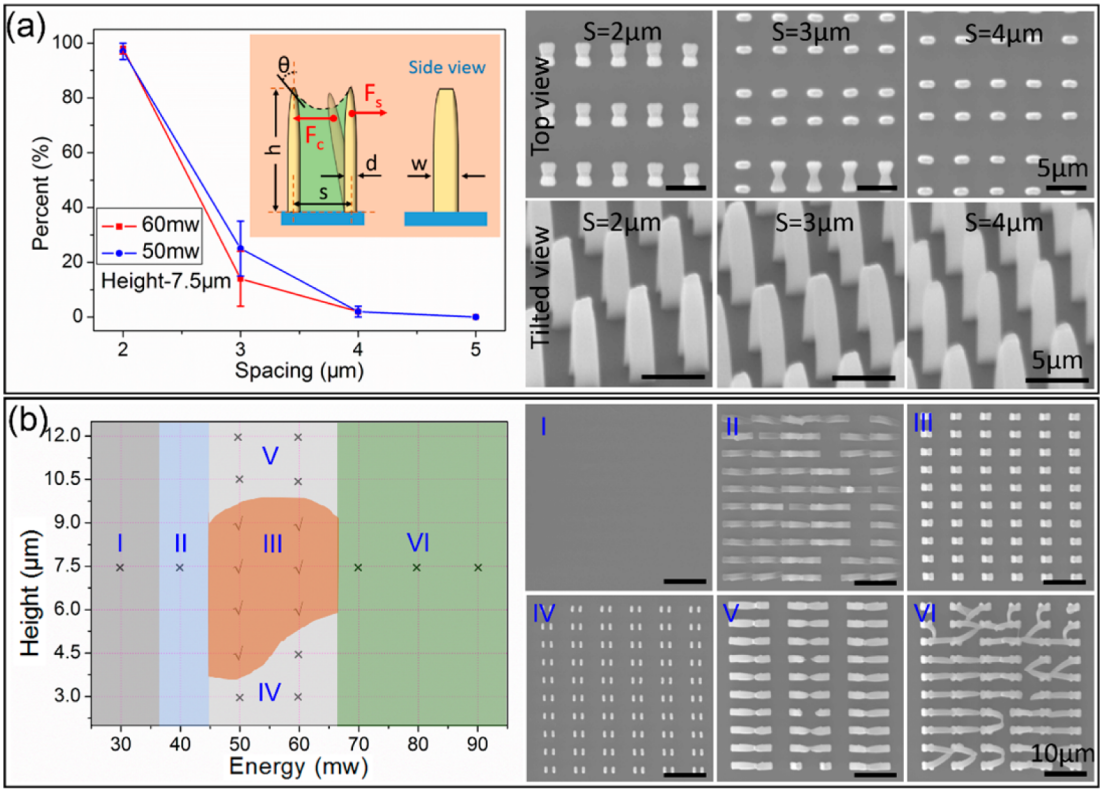

Figure 2. Controllable LPCS. The self-assembled structures are a result of the competition between capillary force and standing force of micropillars. (a) The line chart shows the influence of spacing (*s*) between two pillars processing with 50 and 60 mW, respectively. Inset schematic shows the factors which impact the result of self-assembly: the height (*t*), thickness (*d*), and width (*w*) of a pillar, the spacing (*s*) between two pillars in a cell, and the contact angle (θ) of liquid and pillars. Right SEM images show the assembly results of different *s* varing from 2 to 4 μm with top view and tilted view (45°). The height of pillars in SEM images of (a), whose processing energy is 60 mW, is 7.5 μm. Scale bar: 5 μm. (b) The comprehensive effect of processing energy (lateral axis) and micropillars height (vertical axis) on self-assembly when the spacing is 2 μm. As shown in (b), the graph is divided into six regions in which only a suitable combination of laser power and pillars height is able to ensure homogeneous self-assemblies (region III). The right SEM images represent six regions in the graph, respectively, from which we can learn that uniform self-assemblies cannot be achieved due to inappropriate laser power or pillars height. Scale bar: 10 μm.

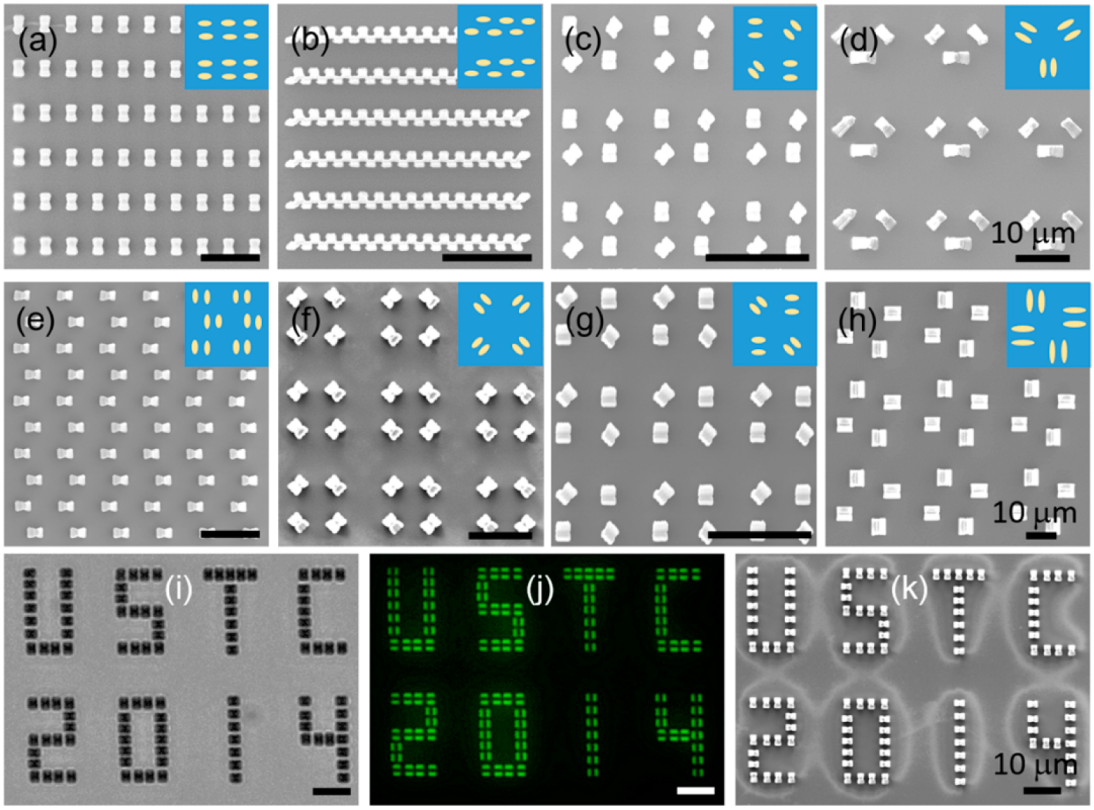

Figure 3. Diverse ordered structures prepared by the LPCS approach. (a–h) Different patterns of cells constructed by two ellipse micropillars, inserts are corresponding schematic diagrams of the design of the micropillars. (i–k) Optical (i), fluorescence (j), and SEM (k) images of the "USTC 2014" pattern. Scale bar: 10 μm.

The distance between two individual cells is designed two times larger than the internal spacing in a cell, so that the influence between two cells can be ignored. Meanwhile, the ellipse cross section is simplified as a rectangle with side lengths of d and w. As the developer evaporates to the level of the freestanding tips, a meniscus is formed between neighboring pillars, yielding a capillary force along the direction of the short axis:[1]

$$F_c \sim \frac{hw\gamma \cos\theta}{s} \quad \ldots \qquad (1)$$

which is proportional to the interfacial tension γ of the solvent, the height h and the width w of pillars, the cosine of contact angle θ, and inversely proportional to the spacing s between adjacent pillars, as shown in Figure 2a. Resistance to the capillary force is the bending ability of pillars, giving rise to an elastic restoring force upon contact at their tips:

$$F_s \sim E\frac{d^3ws}{h^3} \quad \ldots \qquad (2)$$

where E is the Young's modulus, h is the height of the pillars, d and w are short and long axis of cross section of micropillar, respectively, and s is spacing between adjacent pillars. (More details about the calculation of F_c and F_s can be seen in Figure S1.) It is obvious that the elastic force along short axis is much smaller than that along long axis owing to the anisotropic cross section $w > d$, implying that the pillars will easily bend in the direction of short axis.

When $F_c > F_s$, the pillars will collapse and assemblies will be finally formed. To direct the self-assembly as desired, it is necessary to finely tune the relationship between the capillary and elastic forces. As shown in Figure 2a, the spacing s between two pillars is a critical factor that impacts collapse. When s is 2 μm and h is 7.5 μm, almost all pillars will collapse despite the fabrication power is either 60 mW or 50 mW. But the success rate reduces to <30% when s is increased to 3 μm. Few pillars can collapse successfully when s is larger than 4 μm. Making s equal to 2 μm, we can get statistic results on yield ratio by adjusting the height of pillars and power of fs-laser. As shown in Figure 2b, the graph is divided into six regions in which only a certain combination of laser power and pillars height can ensure homogeneous self-assemblies (region III). Otherwise, uniform self-assemblies cannot be achieved due to inappropriate laser power or pillars height.

Because of the high flexibility of fs-laser printing, the spatial position of pillars can be easily controlled which leads to diverse ordered patterns as shown in Figure 3a–h (more examples can be found in Figures S2–S4). Especially, when the aspect ratio of pillars cross section increases, the difference between

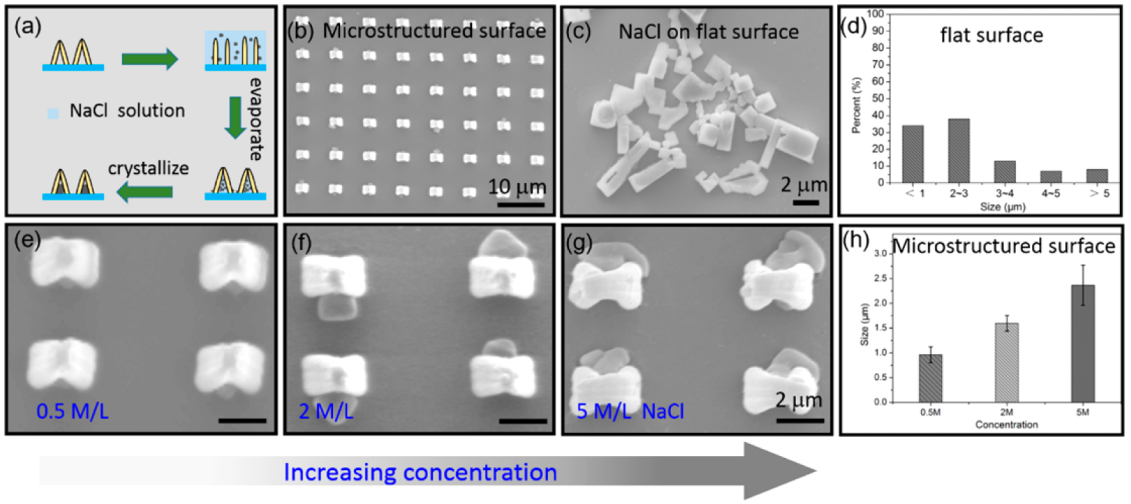

Figure 4. Application of capillary-force driven self-assembled structures in crystallizing microparticles. (a) Schematic diagrams of solution-evaporation self-assembly induced by micropillar cells. NaCl micro/nanoparticles grow inside the cells. (b) Particle array is obtained in this method. (c) NaCl solution evaporates on flat surface, leaving irregular crystals. (d) The size distribution of NaCl crystal in (c). (e–g) Magnified SEM images of NaCl particles grown in cells. The concentrations of self-assembly mother solution are 0.5, 2 , and 5 M/L, respectively. (h) The size of crystallized particles increases with the concentration. It is worth noting that, as shown in (g), the upper part of the micropillars is bent (Figure S9) when concentration is high enough, suggesting that the further collapsing process is hindered by microparticles crytallized from solution left between two pillars. Scale bar: (b) 10 μm; (c, e, f, g) 2 μm.

F_c and F_s also increases, leading to an easier collapse of two pillars which can make up a long hollow channel as shown in Figure 3h. It is a simple method to manufacture hollow channel which may be used in the field of microfluidic chips.[4] Figure 3i–k is the optical, fluorescence and SEM images of a pattern "USTC 2014", respectively, demonstrating the favorable designability of the laser printing capillary-assisted self-assembly (LPCS) method.

Controllable Crystallization of NaCl Microparticles by the Self-Assembled Micropillars Structures. So far, we have shown that diverse patterns and large-scale structures can be assembled by anisotropic micropillars with LPCS method. Next, we will show that these self-assembled structures can be used to induce solution-evaporation self-assembly by which micro/nanoparticles and even microlines can be ultimately produced. Micro/nanoparticles are a kind of special microstructures that have a lot of applications in fields ranging from drug delivery[41,42] to chemical catalysis.[43] Conventional ways to prepare microscale particles mainly include physical grinding and chemical reaction generation which are labor intensive or produce toxic. As a simple and convenient approach, solution-evaporation self-assembly induced by microstructure morphology has been proved to be a promising method thus attracted more and more attentions.[30] But chemical modification involved in this method increases the complexity and cost of experiments. Therefore, simpler methods remain desired for preparation of microparticles. In our previous work, capillary-assisted self-assembled structures are used only as tools to trap and release micro-objects. Here we further develop them in growing microparticles combined with solution-evaporation self-assembly.

The controllable growth procedure of NaCl microparticles is sketched in Figure 4a. Assembled pillars without any chemical modification will unfold when NaCl solution and 1-propanol (solution: 1-propanol = 1:1) are dropped on them. As solvent evaporates, the contact line of the droplet shrinks, leaving some liquid only between two pillars of a cell. At the same time, the NaCl concentration becomes more and more high, finally leading to crystallization. As solution continues to evaporate, pillars are assembled once again into ordered structures with NaCl microparticles grown in the cells. As shown in Figure 4b, there are self-assembled particles in almost every cell, demonstrating good reliability of this method (Figures S5–S6). In comparison, solution-evaporation self-assembly on flat surface is also performed with the same condition. NaCl crystal grows on flat surface (Figure 4c) whose size distribution is counted in Figure 4d. It can be seen that crystal grown on flat surface is disorderly and irregular.

In this microstructure induced self-assembly method, the size of particles depends on the concentration of mother solution, parameters of solute, and the solution volume left in each cell. From the SEM images, we can find that the shapes of particles growing in cells are not standard spherical. So, the size of the particles is difficult to measure precisely because of their irregular shape. However, due to the surface tension induced by solvent evaporation, the shape of most particles is approximate to round or elliptical (Figure S5c). Therefore, in order to simplify the measurement, we estimate the size of particles by measuring the diameter in top-view SEM

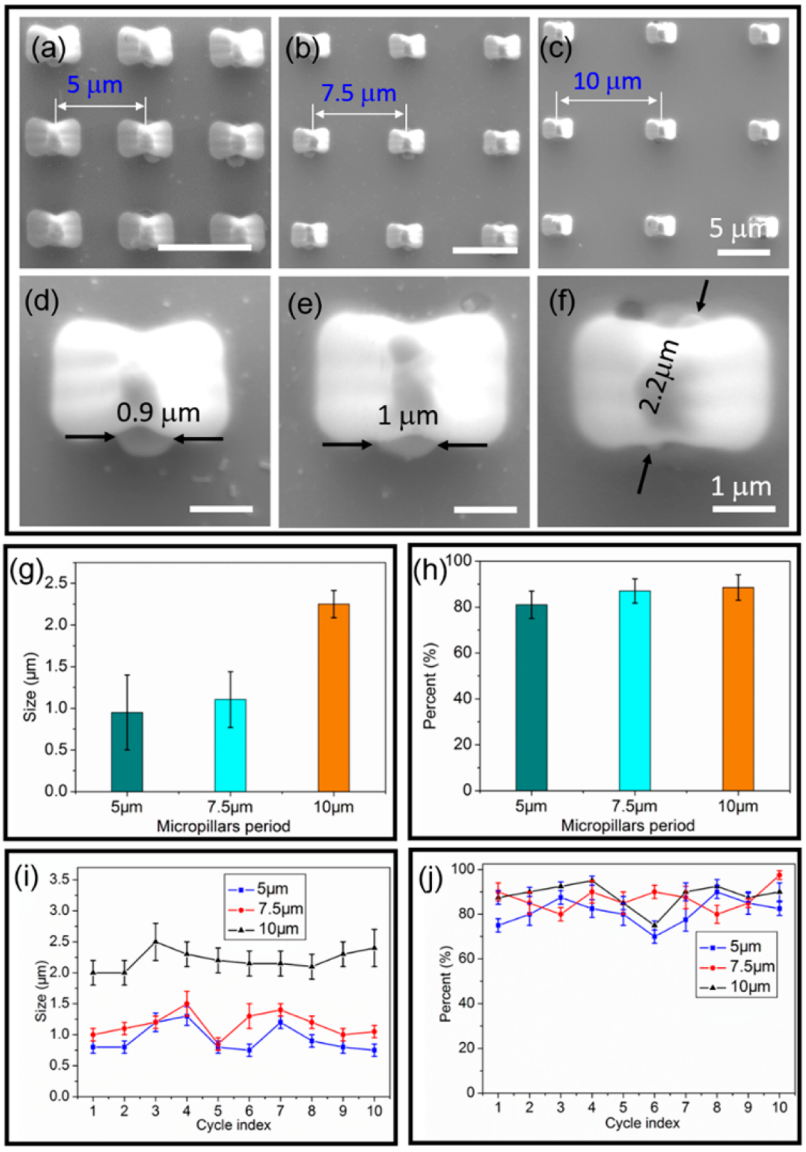

Figure 5. Different patterned crystal arrays in micropillar cells. The internal pillar spacings in cells are all 2.5 μm while the cell periods are 5 μm (a, d), 7.5 μm (c, e), 10 μm (d, f), respectively. The concentrations of the crystallization mother solution are all 0.5 M/L. (g) The sizes of NaCl microparticles generated in pillar cells with different periods and (h) is the ratio of NaCl microparticles growing successfully in cells with different periods. Several crystallization-dissolution cycles are performed and the dependence of microparticles size and ratio of success are shown in (i) and (j). Scale bar: (a, b, c) 5 μm; (d, e, f) 1 μm.

images. So, to better discuss the factors that affect the size of particles, the size of particles can be expressed as the following equation:

$$X \sim \frac{V_l M M_r}{\rho} \quad ... \qquad (3)$$

where V_l is the volume of liquid leaving in cells; M is the concentration of mother solution; M_r and ρ are the relative molecular mass and density of solute, respectively. (More can be seen in Figure S7.) The concentration of NaCl solution is tuned from 0.5 to 5 M/L to study the relationship between the size of microparticles and the concentration of mother liquid. As shown in Figure 4e−g, the particles size become bigger with the increasing concentration. From Figure 4h we can learn that the size of particles grown on microstructured surface is much more uniform than that grown on flat surface. It is worth mentioning that different from the assemblies without crystallized particles, only the tip of two pillars collapse to touch each other at higher concentration (>5 M/L) because self-assembled particles hamper the pillars collapsing (Figure S8).

Distribution Density of Micropillar Cells and Dissolve-Evaporate Cycle. In addition to changing concentration of mother solution, we also attempt to tailor the particles size by adjusting distribution of micropillars. From eq 3, we can learn that the volume of liquid leaving in the cells is another crucial factor that determines the size of microparticles. The volume of leaving liquid mainly depends on *s* and *w* of pillars which can be conveniently

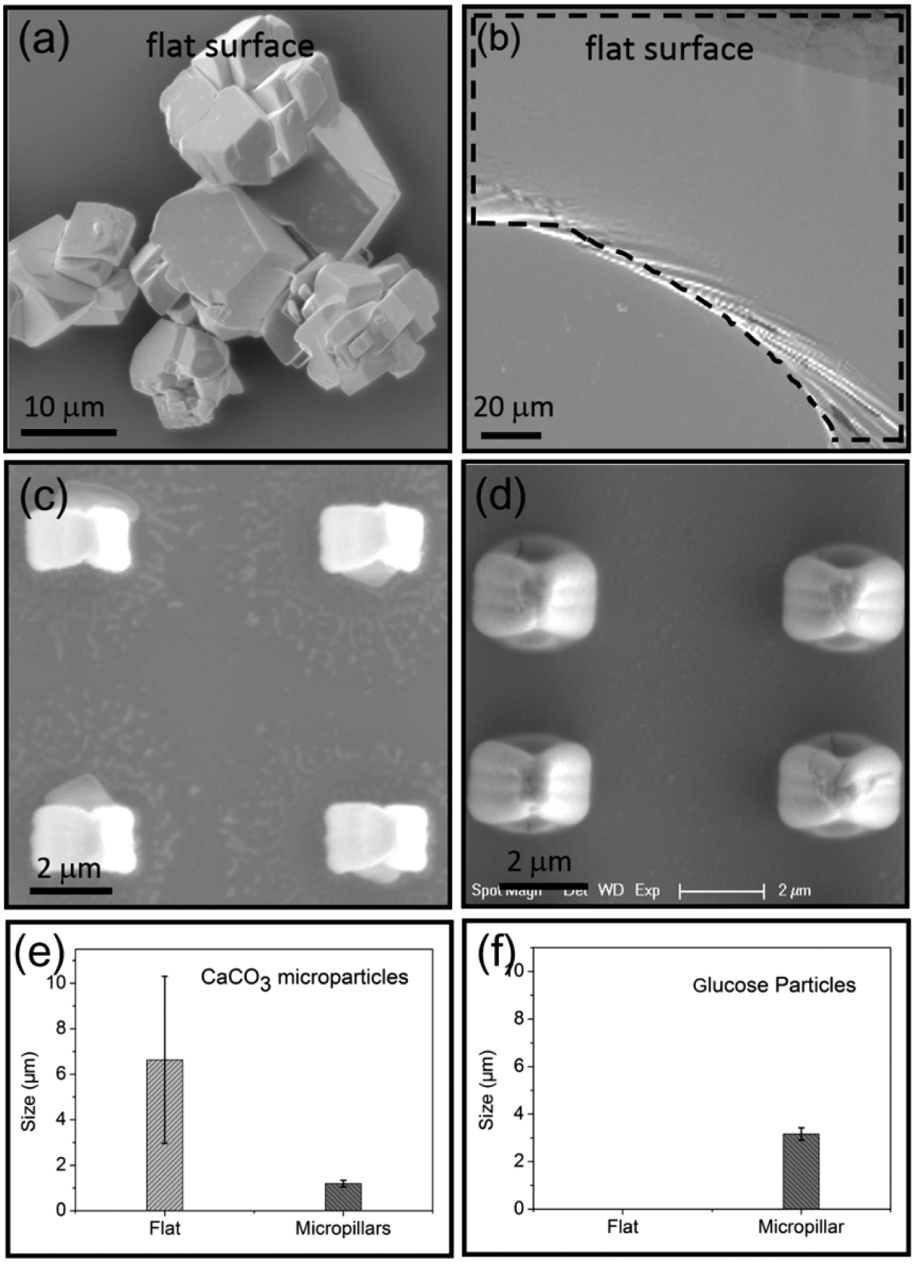

Figure 6. $CaCO_3$ and glucose microparticles are grown in structures induced by solution-evaporation self-assembly method. (a, b) After $CaCO_3$ and glucose solutions evaporating on flat surface, $CaCO_3$ crystal (a) and glucose membrane (b, black dotted area) are left. (c, d) $CaCO_3$ and glucose microparticles are grown inside the cells. (e, f) The sizes of $CaCO_3$ and glucose particles grown on flat/micropillars surface.

tuned in LPCS. However, changing the spacing and width of pillars may cause unexpected failure of assemblies. As shown in Figure 2a, the ratio of success of capillary force driven self-assembly rapidly decreases when *s* is larger than 2 μm. An interesting phenomenon we observed is that microparticles tend to grow in cells which assembled successfully rather than those did not collapse (Figure S9). Therefore, we define the density of cells that the number of two-pillars per area which is inversely proportional to the period of cells. During shrinking process of the microdroplet on substrate, solution leaves around pillars as well as inside the two pillars in a cell. Therefore, we investigate the dependence of the particles size on the cell density. Figure 5a–f shows SEM images of particles growing in cells with distribution spacing changing of 5, 7.5, and 10 μm. Figure 5g exhibits that particles size increases along with the micropillars period. We define a factor *R* as the ratio of the number of pillar cells which generate crystallized particles to that of total number. Figure 5h shows the dependence of *R* on the micropillars period, suggesting that the ratio of success increases slightly with the micropillars period. Interestingly, by adjusting the distance between cells and the concentration of mother solution, NaCl microlines can be gained on microstructure surface (Figure S10). On the whole, growing

microparticles by structure induced solution-evaporation self-assembly is a method of high reliability.

Furthermore, particles can be dissolved and washed away by adding solution that can dissolve the microparticles. Then, a series of crystallization-dissolution cyclic experiments are taken. Figure 5i,j presents the sizes of generated particles and success rates of growing in different cycles. Figure 5 shows that a growth trend corresponding to the increase of the period and the relationship between success and period is not significant. Moreover, by adding solution that cannot dissolve particles, the assembled pillars will open, and the microparticles can be thus washed away (Figure S11).

$CaCO_3$ and Glucose Particles Growing in Cells. We have demonstrated that capillary driven self-assembly structures can be utilized to induce solution-evaporation self-assembly of uniform microscale NaCl particles. Next, we further show that our method for producing particles is applicative for not only soluble materials but also others with poor water-solubility, regardless of organic or inorganic.

Because of their excellent biocompatibility and biodegradability, $CaCO_3$ particles have been investigated as vessels for drug capture and release.[31,44] However, there are few approaches to control spatial position of $CaCO_3$ growth and deposition from solution on surface. Though a method by which $CaCO_3$ can grow on the tip of post from solution has been proposed by Hatton, B. D. and Aizenberg, J., it also requires multistep lithography and complex chemical modification. Moreover, glucose is an intermediate product of metabolism and main energy source of living cells which can be directly absorbed and used to supplement the heat of body. Therefore, glucose microparticles may be widely used in the field of cell culture chips.

Based on the microstructure induced solution-evaporation self-assembly, $CaCO_3$ and glucose microparticles can be conveniently manufactured, as shown in Figure 6a–d. There are irregular $CaCO_3$ crystals and glucose film left rather than microparticles after solution evaporates on flat surface. It should be noted that the glucose particles will swell under irradiation of electron beam of SEM (Figure 6d, 5 keV). $CaCO_3$ and glucose particle sizes in Figure 6a–d were counted in Figure 6e, f, respectively, from which we can see that the sizes of particles on micropillars surface are uniform, while those on flat surface are decentral. An interesting phenomenon worth mentioning is that glucose microlines can be generated on micropillar structured surface when the concentration of glucose solution increased (Figure S12). And when concentration is extremely high, glucose film will also be produced on micropillar surface. We believe that the simplicity, convenience, and universality of our method will make it a competitive candidate for microparticles preparation.

CONCLUSION

In summary, we have demonstrated a new method for realizing hierarchical periodic microstructures which combines fs-laser printing anisotropic pillars with capillary force driven self-assembly. The cross section of micropillar is designed to be anisotropic ellipse to direct the capillary force and the subsequent collapse. Various microarchitectures are designed and constructed by tuning competition through spatial arrangements and pillar heights, respectively. Complicated assemblies can be achieved due to the high flexibility of this method. Comparing with other conventional approaches such as UV photolithography,[2,23] electron beam lithography,[3,24] multibeam interference,[9] and template replicating,[45] this top-down/bottom-up hybrid strategy for preparing hierarchical structures features simplicity, scalability, and high flexibility. Moreover, the assembled cells can be used to induce solution-evaporation self-assembly of a variety of microparticles. The distribution density of the micropillar arrays or the concentration of the crystallization mother liquid is tunable in order to finely control the size of self-assemblied microparticles. NaCl, $CaCO_3$, and glucose microparticles are gained between micropillars, suggesting this method is universal. This method which combined fs-laser printing with capillary force and solution-evaporation self-assembly technology opens a new gallery to fabricate novel 3D microstructures and micro/nanoparticles of different materials and may find numerous applications in the communities of chemistry, biomedicine, and microfluidic engineering.

EXPERIMENTAL SECTION

LPCS Fabrication of Micropillar Arrays. To produce micropillar arrays, we employ a typical femtosecond laser direct writing system, in which a Ti:sapphire laser oscillator (Chameleon vision-S, Coherent) is used as the light source, whose repetition rate is 80 MHz with a pulse duration of 75 fs. The fs-laser in processing working at a central wavelength of 800 nm. A 50× objective (Olympus, NA = 0.8) is used to focus the laser beam inside the photoresist. A commercially available zirconium-silicon hybrid sol–gel material is used for photopolymerization (SZ2080, provided by IESL-FORTH, Greece). The detailed information about two photon polymerization can be seen elsewhere.[46–48] The principal advantage of this material in comparison to other photoresists is the negligible shrinkage during structuring. After polymerization, the sample is developed in 1-propanol for 40 min until all the unpolymerized parts are washed away. After extracting from 1-propanol, the micropillars array will self-assemble into highly ordered structures with the aid of accompanying capillary force during the subsequent evaporation of the liquid layer left on the sample surface.

Sample Characterization. The structures of the pillar-structured silicon substrates and patterning unit arrays were investigated using SEM (FEI, Sirion 200) at an accelerating voltage of 5.0, 10.0,

or 15.0 kV. A Leica fluorescence microscopy (LEICA DMI3000 B) was employed to get the optical and fluorescent images.

Solution-Evaporation Self-Assembly. The self-assembly mother liquids is prepared by dissolving the aimed material in aqueous solutions in a beaker. The concentration of NaCl solutions is 0.5/2/5 mol/L, respectively, to tailor the size of the crystals. In a typical patterning crystal-array fabrication process, a NaCl solution droplet (approximately 2 μL) is dropped onto micropillar arrays, forming a crescent shape on the slide. Then, a 1-propanol (about 2 μL) droplet is dropped to make the solution spreading on the slide. The environment condition is kept 23 $\pm$ 1 °C in 45 $\pm$ 5% relative humidity. Some solution will be left in the self-assembled microunit during the shrinking of edge of the droplet when it evaporates. Owing to the evaporation of solution, microcrystals grow between two micropillars of a cell. $CaCO_3$ solution is prepared by dissolving excessive $CaCO_3$ in deionized water at 23 °C. Common edible glucose is dissolved in deionized water, whose concentration is about 20 mM/L. The glucose crystals grow between micropillars and expand to spherical when irradiated by 5 kV electron beam of SEM.

Conflict of Interest: The authors declare no competing financial interest.

Acknowledgment. This work is supported by National Science Foundation of China (nos. 51275502, 61475149, 51405464, 91223203, and 11204250), Anhui Provincial Natural Science Foundation (no. 1408085ME104), National Basic Research Program of China (no. 2011CB302100), the Fundamental Research Funds for the Central Universities, and "Chinese Thousand Young Talents Program".

Supporting Information Available: The Supporting Information is available free of charge on the ACS Publications website at DOI: 10.1021/acsnano.5b04914.

Experimental details and data (PDF)

REFERENCES AND NOTES

1. Wu, D.; Chen, Q. D.; Xu, B. B.; Jiao, J.; Xu, Y.; Xia, H.; Sun, H. B. Self-Organization of Polymer Nanoneedles into Large-Area Ordered Flowerlike Arrays. *Appl. Phys. Lett.* **2009**, *95*, 091902.
2. Feiertag, G.; Ehrfeld, W.; Freimuth, H.; Kolle, H.; Lehr, H.; Schmidt, M.; Sigalas, M. M.; Soukoulis, C. M.; Kiriakidis, G.; Pedersen, T.; Kuhl, J.; Koenig, W. Fabrication of Photonic Crystals by Deep X-ray Lithography. *Appl. Phys. Lett.* **1997**, *71*, 1441.
3. Hu, W.; Sarveswaran, K.; Lieberman, M.; Bernstein, G. H. Sub-10 nm Electron Beam Lithography Using Cold Development of Poly (methylmethacrylate). *J. Vac. Sci. Technol., B: Microelectron. Process. Phenom.* **2004**, *22*, 1711.
4. Enkrich, C.; Pérez-Willard, F.; Gerthsen, D.; Zhou, J. F.; Koschny, T.; Soukoulis, C. M.; Wegener, M.; Linden, S. Focused-Ion-Beam Nanofabrication of Near-Infrared Magnetic Metamaterials. *Adv. Mater.* **2005**, *17*, 2547.
5. Leong, T. G.; Zarafshar, A. M.; Gracias, D. H. Three-Dimensional Fabrication at Small Size Scales. *Small* **2010**, *6*, 792–806.
6. Randhawa, J. S.; Laflin, K. E.; Seelam, N.; Gracias, D. H. Microchemomechanical Systems. *Adv. Funct. Mater.* **2011**, *21*, 2395–2410.
7. Jacobs, H. O.; Tao, A. R.; Schwartz, A.; Gracias, D. H.; Whitesides, G. M. Fabrication of a Cylindrical Display by Patterned Assembly. *Science* **2002**, *296*, 323–325.
8. Noorduin, W. L.; Grinthal, A.; Mahadevan, L.; Aizenberg, J. Rationally Designed Complex, Hierarchical Microarchitectures. *Science* **2013**, *340*, 832.
9. Wu, D.; Wu, S. Z.; Zhao, S.; Yao, J.; Wang, J. N.; Chen, Q. D.; Sun, H. B. Rapid, Controllable Fabrication of Regular Complex Microarchitectures by Capillary Assembly of Micropillars and Their Application in Selectively Trapping/Releasing Microparticles. *Small* **2013**, *9*, 760–767.
10. Hsu, J. W. P.; Tian, Z. R.; Simmons, N. C.; Matzke, C. M.; Voigt, J. A.; Lui, J. Directed Spatial Organization of Zinc Oxide Nanorods. *Nano Lett.* **2005**, *5*, 83.
11. Xia, Y.; Yin, Y.; Lu, Y.; McLellan, J. Template-Assisted Self-Assembly of Spherical Colloids into Complex and Controllable Structures. *Adv. Funct. Mater.* **2003**, *13*, 907.
12. Xin, Z. Q.; Su, B.; Wang, J. J.; Zhang, X. Y.; Zhang, Z. L.; Deng, M. M.; Song, Y. L.; Jiang, L. Continuous Microwire Patterns Dominated by Controllable Rupture of Liquid Films. *Small* **2013**, *9*, 722–726.
13. Leong, T. G.; Randall, C. L.; Benson, B. R.; Bassik, N.; Stern, G. M.; Gracias, D. H. Tetherless Thermobiochemically Actuated Microgrippers. *Proc. Natl. Acad. Sci. U. S. A.* **2009**, *106*, 703–708.
14. Gultepe, E.; Randhawa, J. S.; Kadam, S.; Yamanaka, S.; Selaru, F. M.; Shin, E. J.; Kalloo, A. N.; Gracias, D. H. Biopsy with Thermally-Responsive Untethered Microtools. *Adv. Mater.* **2013**, *25*, 514–519.
15. Breger, J. C.; Yoon, C.; Xiao, R.; Kwag, H. R.; Wang, M. O.; Fisher, J. P.; Nguyen, T. D.; Gracias, D. H. Self-Folding Thermo-Magnetically Responsive Soft Microgrippers. *ACS Appl. Mater. Interfaces* **2015**, *7*, 3398–3405.
16. Stendahl, J. C.; Rao, M. S.; Guler, M. O.; Stupp, S. I. Intermolecular Forces in the Self-Assembly of Peptide Amphiphile Nanofibers. *Adv. Funct. Mater.* **2006**, *16*, 499–508.
17. Sidorenko, A.; Krupenkin, T.; Taylor, A.; Fratzl, P.; Aizenberg, J. Reversible Switching of Hydrogel-Actuated Nanostructures into Complex Micropatterns. *Science* **2007**, *315*, 487.
18. Leong, T. G.; Lester, P. A.; Koh, T. L.; Call, E. K.; Gracias, D. H. Surface Tension-Driven Self-Folding Polyhedra. *Langmuir* **2007**, *23*, 8747–8751.
19. Cho, J.-H.; James, T.; Gracias, D. H. Curving Nanostructures Using Extrinsic Stress. *Adv. Mater.* **2010**, *22*, 2320–2324.
20. Leong, T. G.; Benson, B. R.; Call, E. K.; Gracias, D. H. Thin Film Stress Driven Self-Folding of Microstructured Containers. *Small* **2008**, *4*, 1605–1609.
21. Randhawa, J. S.; Keung, M. D.; Tyagi, P.; Gracias, D. H. Reversible Actuation of Microstructures by Surface-Chemical Modification of Thin-Film Bilayers. *Adv. Mater.* **2010**, *22*, 407–410.
22. Solovev, A. A.; Xi, W.; Gracias, D. H.; Harazim, S. M.; Deneke, C.; Sanchez, S.; Schmidt, O. G. Self-Propelled Nanotools. *ACS Nano* **2012**, *6*, 1751–1756.
23. Jamal, M.; Zarafshar, A. M.; Gracias, D. H. Differentially Photo-Crosslinked Polymers Enable Self-Assembling Microfluidics. *Nat. Commun.* **2011**, *2*, 527.
24. Choi, S.; Yan, M.; Adesida, I. Fabrication of Triangular Nanochannels Using the Collapse of Hydrogen Silsesquioxane Resists. *Appl. Phys. Lett.* **2008**, *93*, 163113.
25. Chandra, D.; Yang, S. Capillary-Force-Induced Clustering of Micropillar Arrays: Is It Caused by Isolated Capillary Bridges or by the Lateral Capillary Meniscus Interaction Force? *Langmuir* **2009**, *25*, 10430–10434.
26. Chandra, D.; Yang, S. Stability of High-Aspect-Ratio Micropillar Arrays Against Adhesive and Capillary Forces. *Acc. Chem. Res.* **2010**, *43*, 1080–1091.
27. Duan, H.; Berggren, K. K. Directed Self-Assembly at the 10 nm Scale by Using Capillary Force-Induced Nanocohesion. *Nano Lett.* **2010**, *10*, 3710–3716.
28. Duan, H.; Yang, J. K. W.; Berggren, K. K. Controlled Collapse of High-Aspect-Ratio Nanostructures. *Small* **2011**, *7*, 2661–2668.
29. Pokroy, B.; Kang, S. H.; Mahadevan, L.; Aizenberg, J. Self-Organization of a Mesoscale Bristle into Ordered, Hierarchical Helical Assemblies. *Science* **2009**, *323*, 237–240.
30. Xie, Z. Y.; Li, L. L.; Liu, P. M.; Zheng, F. Y.; Guo, L. Y.; Zhao, Y. J.; Jin, L.; Li, T. T.; Gu, Z. Z. Self-Assembled Coffee-Ring Colloidal Crystals for Structurally Colored Contact Lenses. *Small* **2015**, *11*, 926–930.
31. Hatton, B. D.; Aizenberg, J. Writing on Superhydrophobic Nanopost Arrays: Topographic Design for Bottom-up Assembly. *Nano Lett.* **2012**, *12*, 4551–4557.
32. Su, B.; Wang, S. T.; Ma, J.; Wu, Y. C.; Chen, X.; Song, Y. L.; Jiang, L. Elaborate Positioning of Nanowire Arrays Contributed by Highly Adhesive Superhydrophobic Pillar-Structured Substrates. *Adv. Mater.* **2012**, *24*, 559–564.
33. Wu, Y. C.; Su, B.; Jiang, L.; Heeger, A. J. "Liquid-Liquid-Solid"-Type Superoleophobic Surfaces to Pattern

Polymeric Semiconductors Towards High-Quality Organic Field-Effect Transistors. *Adv. Mater.* **2013**, *25*, 6526–6533.
34. Su, B.; Wang, S. T.; Wu, Y. C.; Chen, X.; Song, Y. L.; Jiang, L. Small Molecular Nanowire Arrays Assisted by Superhydrophobic Pillar-Structured Surfaces with High Adhesion. *Adv. Mater.* **2012**, *24*, 2780–2785.
35. Su, B.; Wu, Y. C.; Tang, Y.; Chen, Y.; Cheng, W. L.; Jiang, L. Free-Standing 1D Assemblies of Plasmonic Nanoparticles. *Adv. Mater.* **2013**, *25*, 3968–3972.
36. Su, B.; Wang, S. T.; Ma, J.; Song, Y. L.; Jiang, L. "Clinging-Microdroplet" Patterning Upon High-Adhesion, Pillar-Structured Silicon Substrates. *Adv. Funct. Mater.* **2011**, *21*, 3297–3307.
37. Cai, J. H.; Chen, S. R.; Cui, L. Y.; Chen, C. C.; Su, B.; Dong, X.; Chen, P. L.; Wang, J. X.; Wang, D. J.; Song, Y. L.; Jiang, L. Temperature-Controlled Morphology Evolution of Porphyrin Nanostructures at an Oil−Aqueous Interface. *Adv. Mater. Interfaces* **2015**, *2*, 1400365.
38. Wu, D.; Niu, L. G.; Wu, S. Z.; Xu, J.; Midorikawa, K.; Sugioka, K. Ship-in-a-Bottle Femtosecond Laser Integration of Optofluidic Microlens Arrays With Center-Pass Units Enabling Coupling-Free Parallel Cell Counting With a 100% Success rate. *Lab Chip* **2015**, *15*, 1515–1523.
39. Wu, D.; Xu, J.; Wu, S. Z.; Niu, L. G.; Midorikawa, K.; Sugioka, K. In-Channel Integration of Designable Microoptical Devices Using Flat Scaffold-Supported Femtosecond-Laser Microfabrication for Coupling-Free Optofluidic Cell Counting. *Light: Sci. Appl.* **2015**, *4*, e228.
40. Hu, Y. L.; Lao, Z. X.; Cumming, B. P.; Wu, D.; Li, J. W.; Liang, H. Y.; Chu, J. R.; Huang, W. H.; Gu, M. Laser Printing Hierarchical Structures With the Aid of Controlled Capillary-Driven Self-Assembly. *Proc. Natl. Acad. Sci. U. S. A.* **2015**, *112*, 6876–6881.
41. Uskokovic, V.; Lee, P. P.; Walsh, L. A.; Fischer, K. E.; Desai, T. A. PEGylated Silicon Nanowire Coated Silica Microparticles for Drug Delivery Across Intestinal Epithelium. *Biomaterials* **2012**, *33*, 1663–1672.
42. Prow, T. W.; Grice, J. E.; Lin, L. L.; Faye, R.; Butler, M.; Becker, W.; Wurm, E. M. T.; Yoong, C.; Robertson, T. A.; Soyer, H. P.; Roberts, M. S. Nanoparticles and Microparticles for Skin Drug Delivery. *Adv. Drug Delivery Rev.* **2011**, *63*, 470–491.
43. Zhang, Z. L.; Che, H. W.; Gao, J. J.; Wang, Y. L.; She, X. L.; Sun, J.; Poernomo, G.; Zhong, Z. Y.; Su, F. B. Shape-Controlled Synthesis of Cu_2O Microparticles and Their Catalytic Performances in the Rochow Reaction. *Catal. Sci. Technol.* **2012**, *2*, 1207–1212.
44. Du, C.; Shi, J.; Shi, J.; Zhang, L.; Cao, S. K. PUA/PSS Multilayer Coated $CaCO_3$ Microparticles as Smart Drug Delivery Vehicles. *Mater. Sci. Eng., C* **2013**, *33*, 3745–3752.
45. Zhang, Y.; Lo, C. W.; Taylor, J. A.; Yang, S. Replica Molding of High-Aspect-Ratio Polymeric Nanopillar Arrays With High Fidelity. *Langmuir* **2006**, *22*, 8595–8601.
46. Ovsianikov, A.; Viertl, J.; Chichkov, B.; Oubaha, M.; MacCraith, B.; Sakellari, I.; Giakoumaki, A.; Gray, D.; Vamvakaki, M.; Farsari, M.; Fotakis, C. Ultra-Low Shrinkage Hybrid Photosensitive Material for Two-Photon Polymerization Microfabrication. *ACS Nano* **2008**, *2*, 2257–2262.
47. Farsari, M.; Chichkov, B. N. Materials Processing: Two-Photon Fabrication. Materials Processing: Two-Photon Fabrication. *Nat. Photonics* **2009**, *3*, 450.
48. Xiong, W.; Zhou, Y. S.; He, X. N.; Gao, Y.; Mahjouri-Samani, M.; Jiang, L.; Baldacchini, T.; Lu, Y. F. Simultaneous Additive and Subtractive Three-Dimensional Nanofabrication Using Integrated Two-Photon Polymerization and Multiphoton Ablation. *Light: Sci. Appl.* **2012**, *1*, e6.